Journal of Volcanology and Geothermal Research 198 (2010) 158–176

Contents lists available at ScienceDirect

Journal of Volcanology and Geothermal Research

journal homepage: www.elsevier.com/locate/jvolgeores

Effect of syneruptive decompression path on shifting intensity in basaltic sub-Plinian eruption: Implication of microlites in Yufune-2 scoria from Fuji volcano, Japan

Yuki Suzuki *, Toshitsugu Fujii

Earthquake Research Institute, Univ. of Tokyo, 1-1-1, Yayoi, Bunkyo-ku, Tokyo, 113-0032, Japan

ARTICLE INFO

Article history:
Received 25 March 2010
Accepted 20 August 2010
Available online 24 September 2010

Keywords:
basaltic Plinian
microlite
crystal size distribution
outgassing
conduit flow

ABSTRACT

To constrain the timing and conditions of syneruptive magma ascent that are responsible for shifting eruption intensity, we have investigated a basaltic sub-Plinian eruption that produced Yufune-2 scoria in Fuji volcano 2200 years ago. We deduced magmatic decompression conditions from groundmass microlite textures, including decompression path (i.e. evolution in decompression rate) and approximate decompression rate, in order to relate them to eruption intensity. The microlites revealed decompression conditions after water saturation at 700–1100 m depth.

The temporal change in scoria size indicates that the magma discharge rate and resultant eruption intensity increased from unit a to unit b, and then declined toward ending units d and e. The overall decompression rate in each eruptive unit has a positive correlation with eruption intensity. The variation in decompression rate was enlarged in the final units, where the maximum remained the same as the peak through the eruption (0.13–0.22 MPa/s for units b and c), while the minimum was 0.025 MPa/s. The large variation here is due to 1) variation in flow velocity across conduit and 2) part of the erupted magma in unit d experienced remarkably slow decompression (0.002–0.003 MPa/s) resulting from decreased overpressure in the reservoir following the major eruption of unit b. Furthermore, crystal size distribution (CSD) of microlites implied that the earliest erupted magma (unit a) had once been decompressed slowly (0.005–0.012 MPa/s), having been arrested by material in the conduit–vent system, which was followed by an increase in decompression rate due to removal of the material at the initiation of the eruption. In addition, the magma that had been ascending slowly before the unit-d eruption may record the increase in decompression rate. This increased rate resulted from being pushed up by the successive magma at the start of that eruption.

Two factors had a major impact on eruption intensity. First, magma decompression rate determined the degree of gas-phase separation from ascending magma. Judging from CSD, different decompression rates had been generated at least at the start of microlite crystallization. The second factor is the conduit radius that, in combination with magma ascent rate, controlled the magma discharge rate. Before the major eruption of unit b, the conduit radius likely increased, as evidenced by xenoliths of basaltic lava and lithic fragments with the same petrography as the xenoliths in unit a. In unit e, the conduit radius decreased through inward development of high-density magma from the conduit margin.

1. Introduction

The syneruptive magma ascent from the reservoir has been receiving attention recently, because different conditions at this stage produce variable eruption styles and intensities, even when magmas contain a similar amount of dissolved water. For felsic magma, Woods and Koyaguchi (1994) proposed that the shift between lava dome formation and Plinian eruption depends on both magma discharge rate, which is controlled by magma ascent rate and conduit radius, and on reservoir overpressure. Therefore, shifting style and intensity should be interpreted in the context of eruption progress. Among these parameters, magma ascent rate has been a major target of petrological and textural study as it can be directly estimated from volcanic ejecta.

Slower ascent generally enhances outgassing (i.e. separation from magma of the gas phase formed in syneruptive decompression) (e.g. Burgisser and Gardner, 2004). This tends to cause more effusive eruption (Pioli et al., 2008, 2009, example of basaltic magma). In high-viscosity felsic magma, bubbles are always coupled with magma. Therefore, outgassing requires permeability development through connection of vesicles (e.g. Eichelberger et al., 1986). In less viscous basaltic magma, decoupling of bubbles and magma, as exemplified by upward segregation of bubbles, occurs rapidly. Basaltic Plinian eruptions, however, are likely to require a coupling between the bubbles and magma to develop the gas pressure necessary for an explosive eruption (e.g. Sable et al., 2006). Viscosity of basaltic magma in syneruptive ascent can be increased greatly by rapid crystallization in high temperature

* Corresponding author. Tel.: +81 3 5841 5746; fax: +81 3 3812 6979.
E-mail addresses: ysuzuki@eri.u-tokyo.ac.jp (Y. Suzuki), fujii@eri.u-tokyo.ac.jp (T. Fujii).

0377-0273/$ – see front matter © 2010 Elsevier B.V. All rights reserved.
doi:10.1016/j.jvolgeores.2010.08.020

magma (e.g. Lofgren, 1980), as pointed in Taddeucci et al. (2004) and Sable et al. (2006). This physical property change may shift outgassing mode from bubble segregation to permeability development. Because of the above known complexities, studies of particular basaltic eruptions are required to verify and improve theoretical models.

Groundmass microlite texture, characterized by crystallinity, number density, crystal form, and crystal size distribution, provide information on subsurface magma behavior (e.g. Cashman, 1992; Cashman and Blundy, 2000; Rutherford and Gardner, 2000; Blundy and Cashman, 2008). Studies on natural ejecta are supported by experimental studies that quantify the kinetics of decompression-induced crystallization (Hammer and Rutherford, 2002; Martel and Schmidt, 2003; Szramek et al., 2006; Suzuki et al., 2007). The past ten years have seen increasing attempts to relate groundmass texture with eruptive style and intensity and to obtain a better picture of magma flow in the conduit for intermediate to felsic magma eruptions (Gardner et al., 1998; Hammer et al., 1999; Hammer et al., 2000; Noguchi et al., 2006; Clarke et al., 2007; Martel and Poussineau, 2007; Suzuki et al., 2007; Castro and Gardner, 2008; Noguchi et al., 2008). On the other hand, basaltic magma eruptions have not been the focus of much study until recently (Taddeucci et al., 2004; Polacci, et al., 2006; Sable et al., 2006; Szramek et al., 2006; Andronico et al., 2009; Erlund et al., 2009). This has resulted in a poor knowledge of natural microlite textures and limitation of textural constraints on magma decompression rates (estimated only in Szramek et al., 2006; Toramaru et al., 2008).

Furthermore, despite all of these efforts including those for felsic magma, some important aspects of syneruptive magma ascent have not been discussed fully. For example, most previous studies have aimed to reveal the average ascent rate of each magma parcel through syneruptive magma ascent, not its ascent path (i.e. evolution in ascent rate, including temporal arrest). If ascent path were known, its comparison with eruption intensity and style would provide novel insight into the conditions and timing that determined the final eruption. Crystallinity, number density and crystal form tend to reflect not only the integrated sum of a decompression event but also decompression path. For example, crystallinity and number density data may tell us time-evolution of nucleation and growth and, thus, decompression path. However, this method requires a series of magmas that followed almost the same decompression path but were quenched at different times. Crystal form may change with time-evolution of magma supersaturation, but individual crystals do not elucidate when the change in supersaturation took place. Instead, crystal size distribution (CSD) can be used to supplement these approaches. CSD holds clues as to ascent path because its shape reflects the history of crystal nucleation and growth (e.g. Marsh, 1998) and the relative time of change is known from crystal size. Because of the time-consuming nature of CSD acquisition, effective use of CSD for basaltic magma eruption is found exclusively in Taddeucci et al. (2004) to date. Fortunately, recent developments in data processing (Jerram and Higgins, 2007) have made it easier to acquire CSDs for a large number of samples from a series of eruptive activities.

The present work focuses on a basaltic sub-Plinian eruption of Fuji volcano, 2200 years ago (eruption of Yufune-2 scoria; Fig. 1), in order to constrain the timing and ascent conditions of syneruptive magma that are responsible for determining eruption intensity. To make this eruption most effective for investigating this problem, we tried to combine microlite textural data with geological records of the eruption progress, under the recognition that shifting intensity should be interpreted in the context of eruption progress. The geological records found in the present study include the opening of the conduit–vent system in view of the presence of lithic fragments, the changing magma discharge rate, and the temporal wane and cease of the eruptive activity. Microlite textures, including CSD, allow us to document the evolution of magma ascent in the conduit through an eruption. For each magma unit, we relate decompression conditions (rate and path) with degree of outgassing so that we can examine whether motion of bubbles relative to magma had a role in changing eruption intensity.

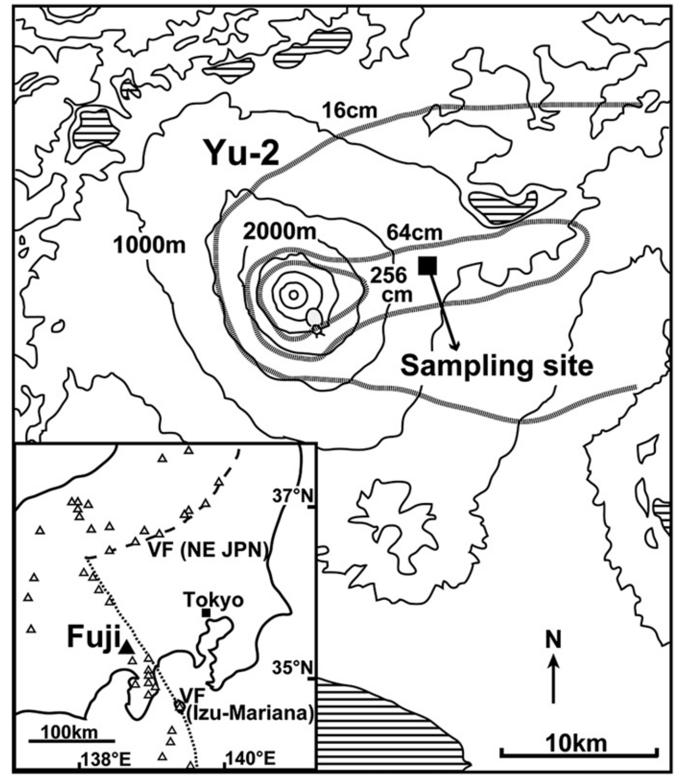

Fig. 1. Isopach map for Yufune-2 scoria (Yu-2) erupted in the last summit eruption of Younger Fuji volcano, with the sampling site in this study. Modified after Miyaji (2007) and Miyaji (1988). Inset shows the location of Fuji volcano in the Izu-Mariana arc. VF (inset), volcanic front.

2. Fuji volcano and Yufune-2 scoria

Mt. Fuji, rising 3776 m above sea level, is one of the largest volcanic edifices in Japan. It is situated at the junction of the Northeast Japan arc and Izu-Mariana arc in central Japan (Fig. 1). Subduction of the Pacific plate beneath the Eurasian plate is the primary process of magma generation. Tsuya (1940) revealed that Mt. Fuji is a composite stratovolcano consisting of Komitake volcano (older than 100 ka), Older Fuji volcano, and Younger Fuji volcano, in decreasing order age. Recent scientific drilling discovered Pre-Komitake volcano (260–160 ka) beneath the Komitake volcano, based on ejecta compositions (Nakada et al., 2007; Yoshimoto et al., 2010). The total volume of ejecta from Fuji volcano (both Older and Younger) reaches 400 km^3. Fuji volcano has issued mostly basaltic magma (e.g. Takahashi et al., 1991; Togashi et al., 1991, 1997; Kaneko et al., 2010), but the basalts are evolved in terms of FeO*/MgO (larger than 1.6) due to high-pressure crystallization (Fujii, 2007). Older Fuji volcano began its activity at nearly the same position as Younger Fuji on the southern slope of the Komitake volcano at 100 ka (Machida, 1964, 2007). The activity of Older Fuji volcano is characterized by ejection of voluminous pyroclastic falls (Uesugi, 1990; Kaneko et al., 2010). Following previous geological study (e.g. Tsuya, 1968), tephrostratigraphy and ^{14}C age determination (e.g. Miyaji, 1988; Yamamoto et al., 2005), Miyaji (2007) divided the activity of Younger Fuji volcano (past 11,000 years) into 5 stages. The activity of Younger Fuji volcano is characterized by changing eruption styles (lava effusion, explosive activities including pyroclastic flow) and eruption locations (summit, flank) at different stages. After the Hoei eruption (AD 1707), no activity has been recorded.

Yufune-2 scoria, the target of the present study, was produced at the end of Stage-4 activity of Younger Fuji volcano (2.2 ka; Miyaji, 1988). The Yufune-2 scoria is one of the wide-spread scoria fall deposits from the summit that characterize Stage-4 activity (3.5–2.2 ka). The eruption style was sub-Plinian throughout and total volume of ejecta reaches 0.5 km^3